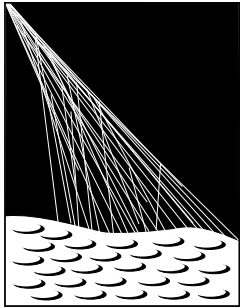


The muon component of extensive air showers above $10^{17.5}$ eV measured with the Pierre Auger Observatory



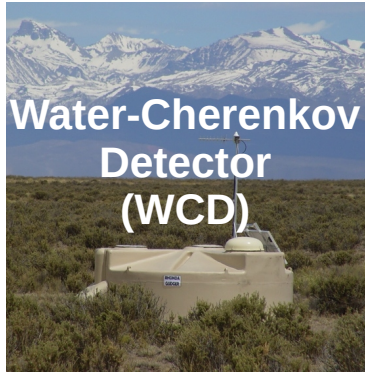
PIERRE
AUGER
OBSERVATORY

Federico Sánchez
for the Pierre Auger Collaboration

36th ICRC 2019

Madison

The Pierre Auger Observatory



Water-Cherenkov
Detector
(WCD)

Surface detector (SD)

100% duty cycle

SD-1500m

3000 km²
1600 WCDs

SD-750m

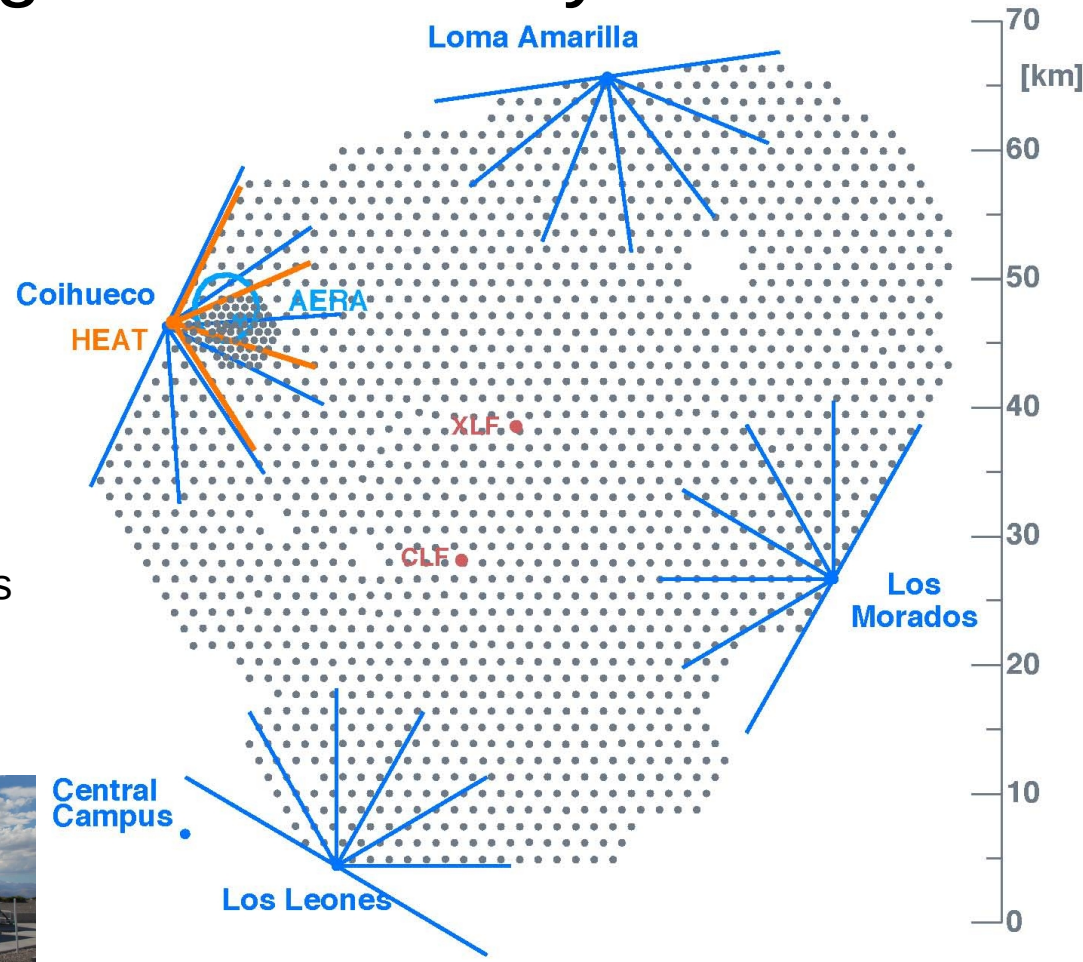
23.5 km²
61 WCDs

Fluorescence detector (FD)

15% duty cycle

4 units x 6 telescopes
overlooking SD-1500m
FoV 30° x 30°
Minimum elevation 1.5°

1 units x 3 telescopes
overlooking SD-750m
FoV 30° x 30°
Minimum elevation 30°



The Pierre Auger Observatory

Underground muon detector (UMD)

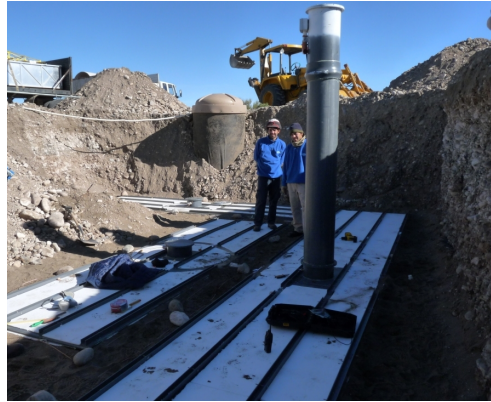
100% duty cycle

UMD-750m

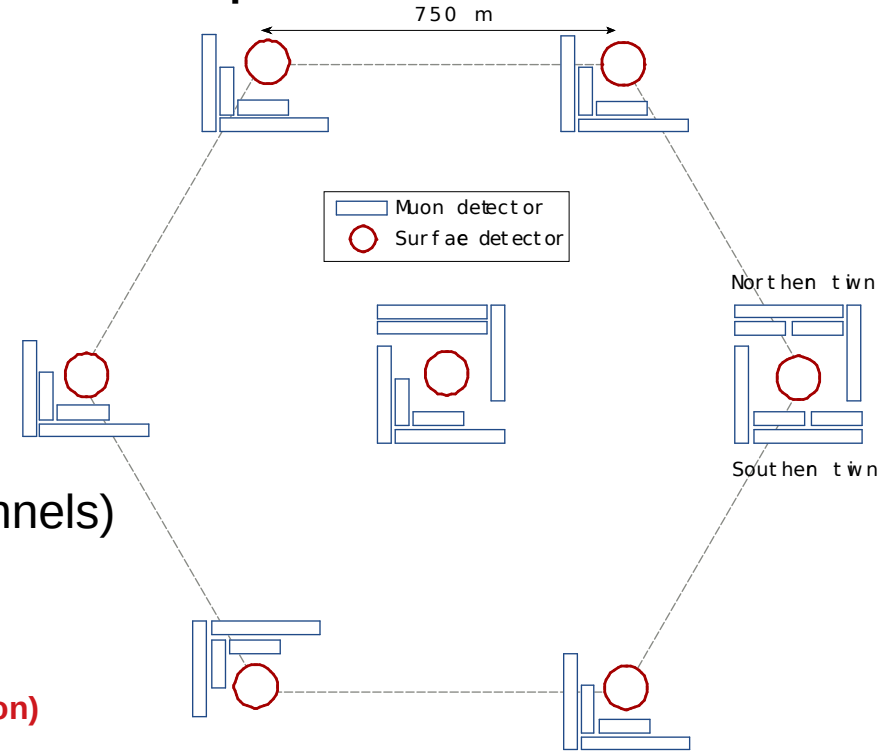
23.5 km²

61x30m² Plastic Scintillators

buried 2.3m triggering from WCDs



Engineering Array: Operated until Nov. 2017



EA served for:

- Validation of detection system (End-to-End)
- Optimization of optical devices (PMT → SiPM)
- Optimization of electronics (ASICs)
- Optimization of dynamic range (2 extra analog channels)

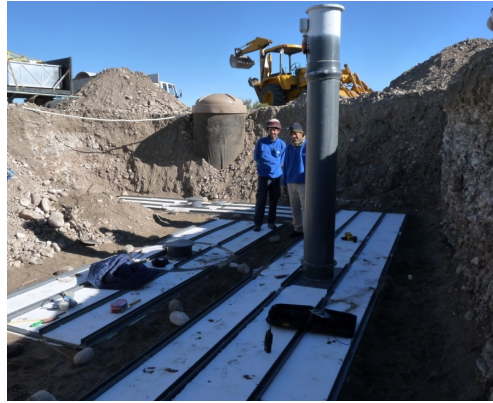
Physics observables are basically extracted from:

- signal size** → **number of muon** (this talk)
- signal timing** → **timing of muon** (see PoS(202) poster session)

1 year of data, 1742 event with energy $3 \times 10^{17} - 2 \times 10^{18}$ eV and zenith angle $< 45^\circ$

UMD: from raw traces to muons

Binary traces in raw (real) events

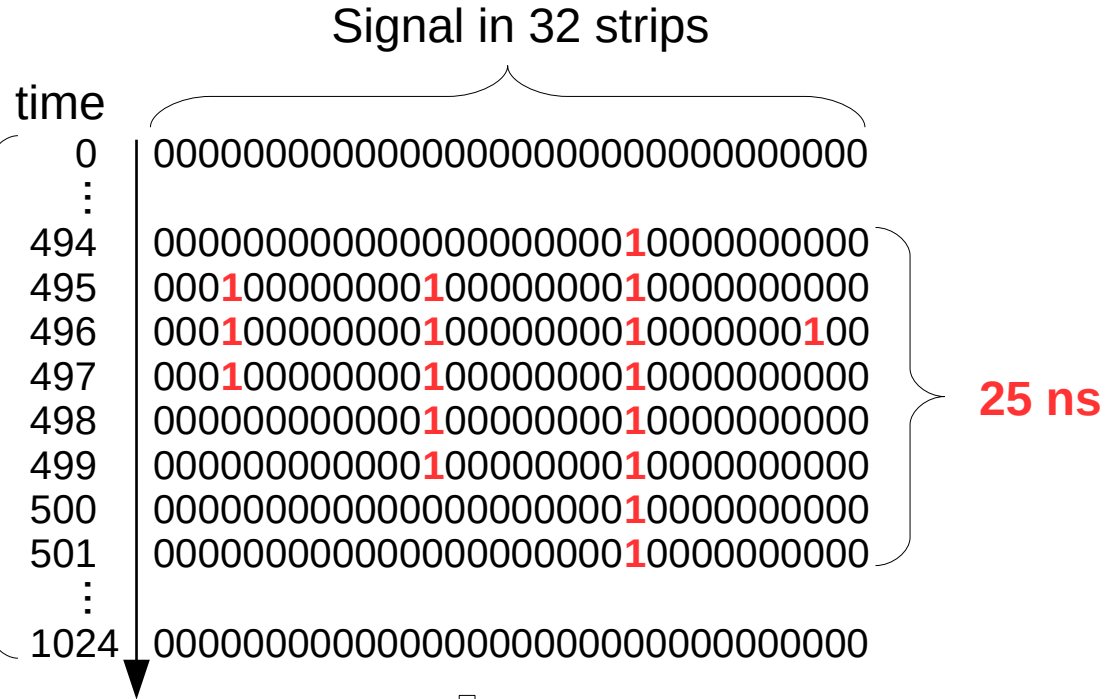


Highly **segmented**
scintillators: 64 per unit



32 strips/side

Sampling @
3.125 ns



3 muons ("111" or "101" minimal pattern required) + 1 noise

UMD: efficiency and resolution

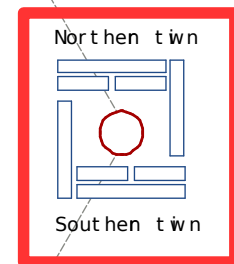
Efficiency
Resolution } based on { \rightarrow units of different areas (5m^2 & 10m^2)
 \rightarrow units of identical areas (30m^2 Vs 30m^2)

Relative efficiency

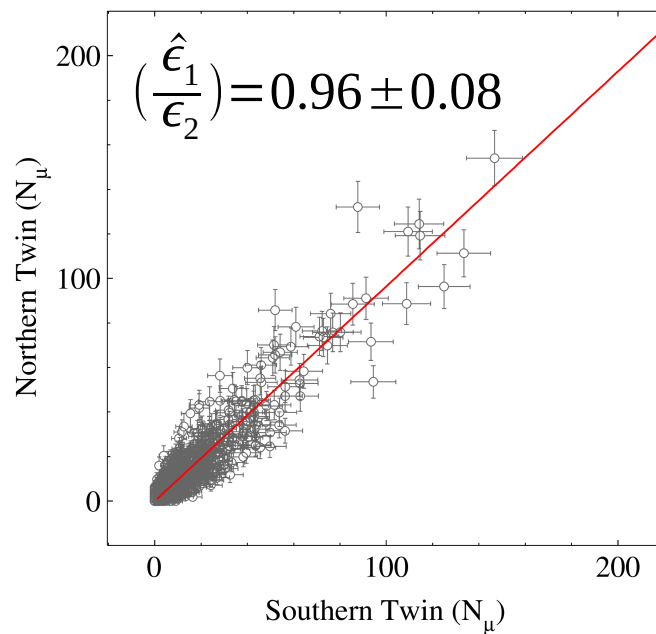
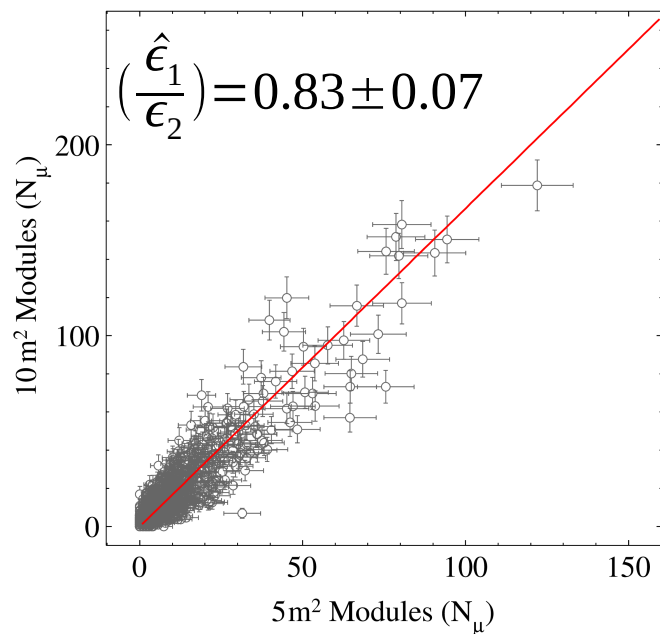
Ratio of counts per unit $r = \frac{\epsilon_1}{\epsilon_2} \cdot \frac{a_1}{a_2}$ } $\rightarrow \left(\frac{\hat{\epsilon}_1}{\epsilon_2} \right) = \frac{a_1}{a_2} \cdot \frac{\langle N_2 \rangle}{\langle N_1 \rangle}$
where ϵ_i, a_i efficiency and area }
Rel. eff. estimator

Twin detectors:

30m^2 North + 30m^2 South of
same WCD highly
segmented (4+4 units)



N-S separation
 $\sim 20\text{ m}$



UMD: efficiency and resolution

Efficiency
Resolution } based on { \rightarrow units of different areas (5m^2 & 10m^2)
 \rightarrow units of identical areas (30m^2 Vs 30m^2)

Resolution

Square ratio of mean
and variance

$$\left(\frac{\sigma}{\langle N \rangle} \right)^2$$

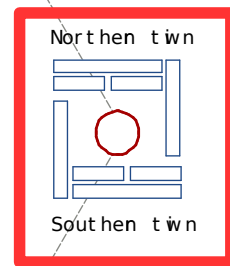
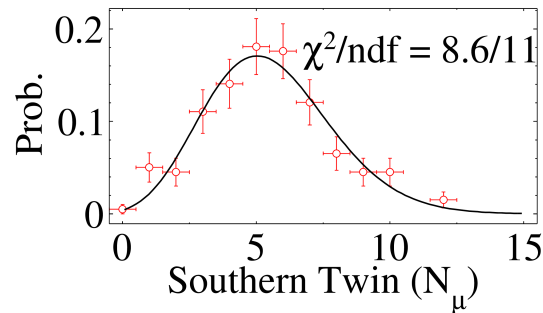
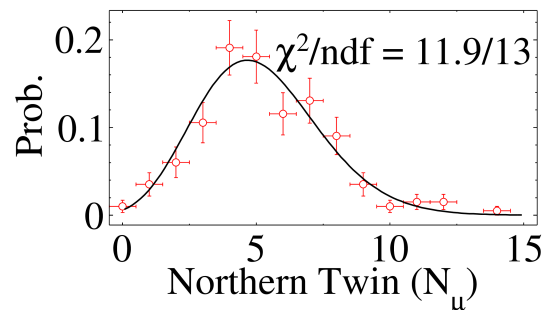
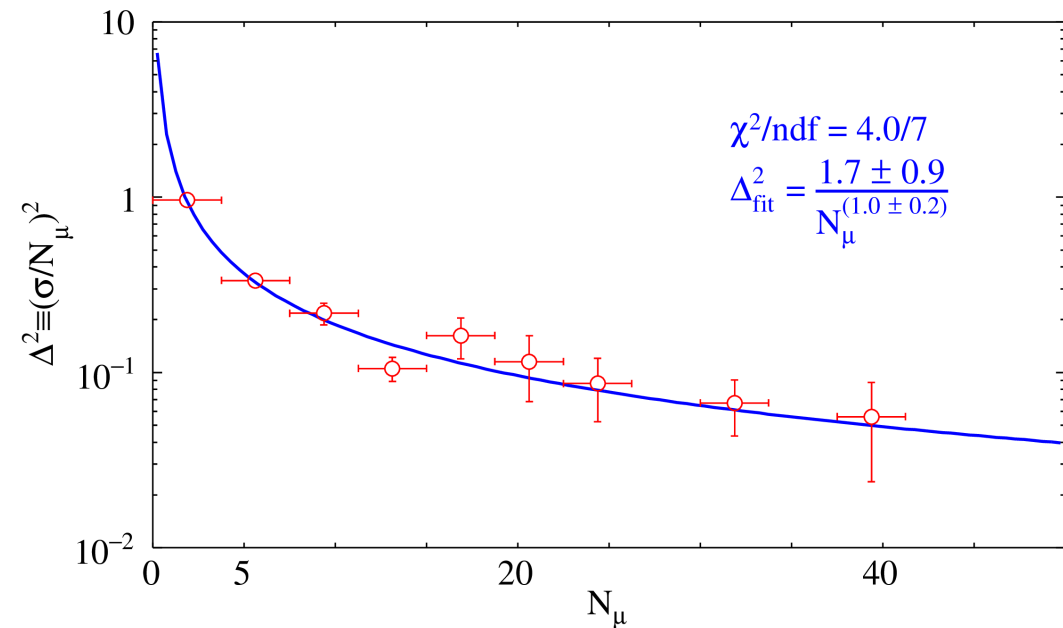


$$\left(\frac{\hat{\sigma}}{\langle N \rangle} \right)^2 = 2 \left(\frac{N_1 - N_2}{N_1 + N_2} \right)^2$$

Resol. estimator

Twin detectors:

30m^2 North + 30m^2 South of
same WCD highly
segmented (4+4 units)



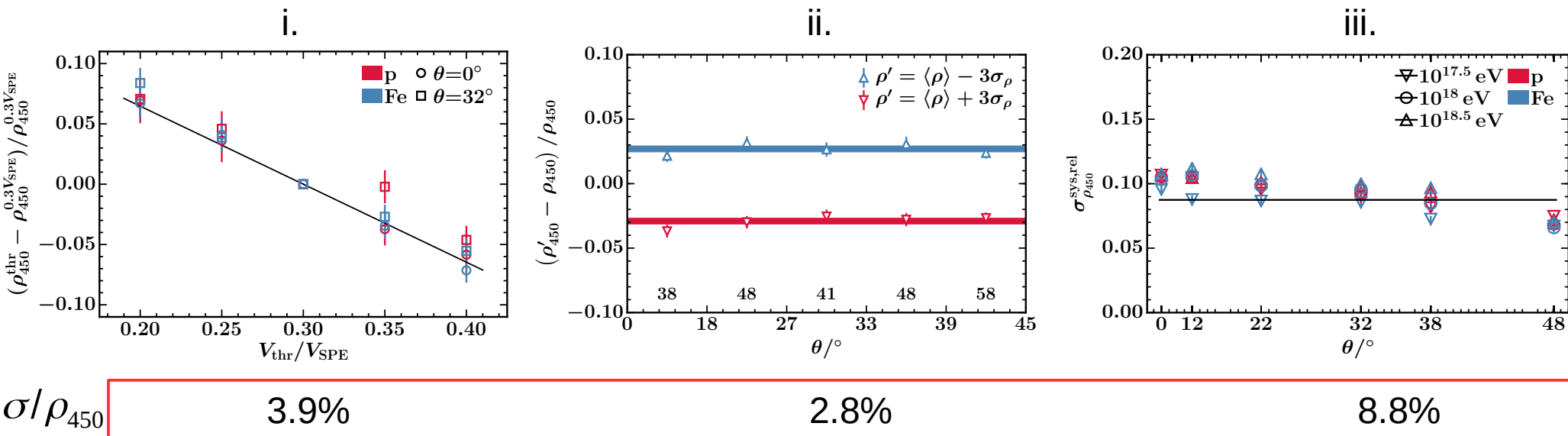
N-S separation
 ~ 20 m

UMD: systematic uncertainties I

Sources of systematic uncertainty analyzed:

- i. Calibration procedure → uncertainty in the “operation” point of each of 2240 electronic channels
- ii. Soil density variations → uncertainty in shielding by overburden
- iii. Shape of muon lateral distribution function → slope $\beta(\theta)$ parametrization based on simulations

Simulation based

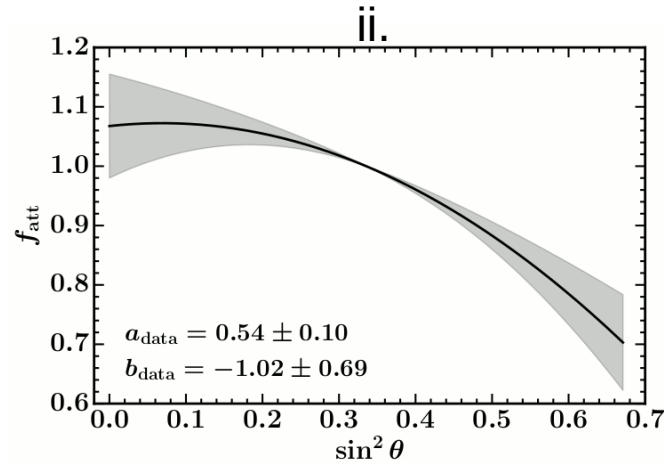
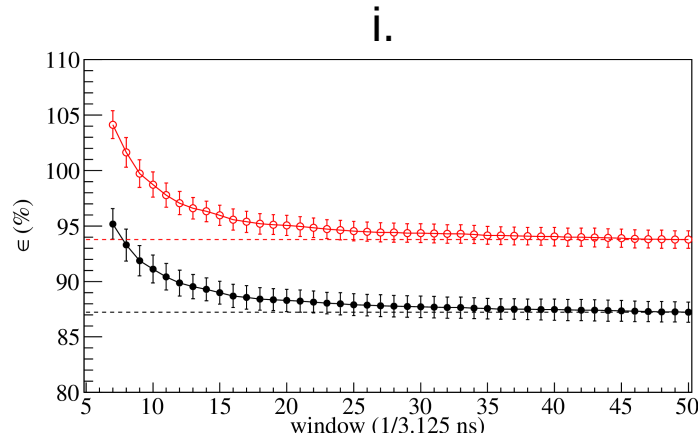


UMD: systematic uncertainties II

Sources of systematic uncertainty analyzed:

- i. Efficiency correction \rightarrow dependent time width selected to identify signals
- ii. Constant Intensity Cut (CIC) correction \rightarrow uncertainty in parametrization

Data based



Total uncertainty:

$$\sigma/\rho_{35} \quad 14.3\%$$

σ/ρ_{450}

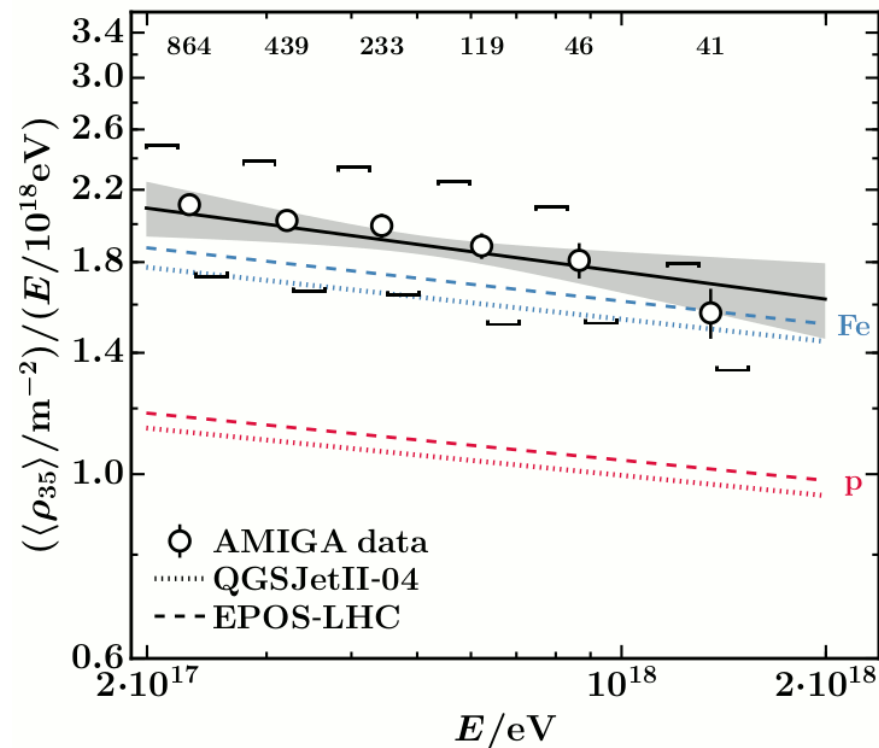
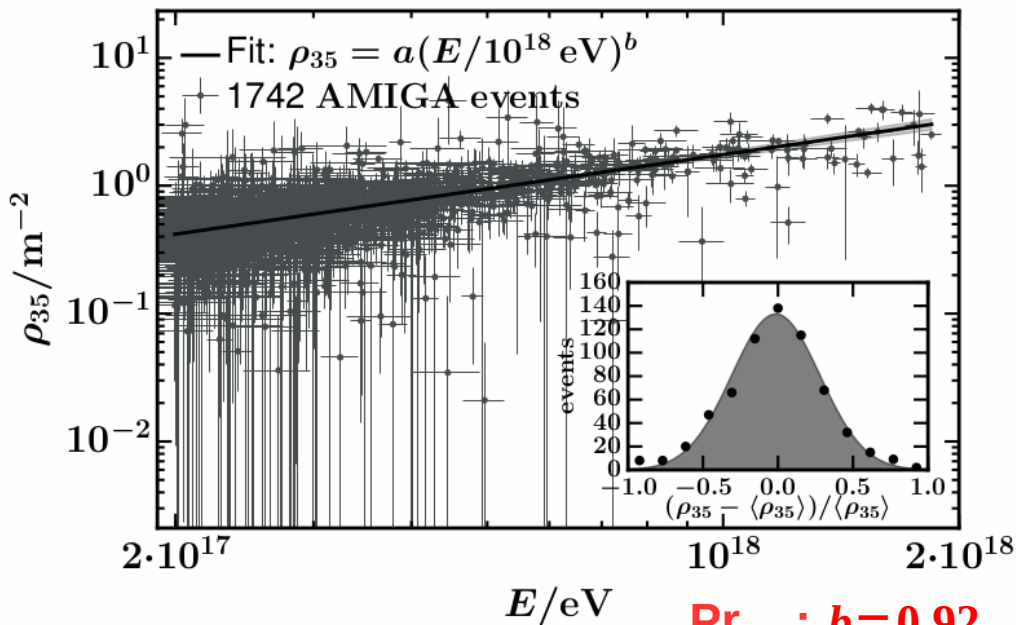
9.9%

2.3%

Muon densities Vs energy $\Rightarrow \rho_{35}(E)$

First direct measurement of the muon densities at energies $10^{17.3} \text{ eV} < E < 10^{18.3} \text{ eV}$

- ✓ Geometry & Energy from SD alone
- ✓ Event core contained in UMD hexagon
- ✓ Zenith $< 45^\circ$



Pr : $b=0.92$

Fe : $b=0.91 \rightarrow 8\% \text{ (EPOS)} - 14\% \text{ (QGSJet)} \text{ below measurements}$

Data: $b=0.89 \pm 0.04 \text{ (stat)} \pm 0.04 \text{ (sys)}$

Comparison with other Auger measurements I

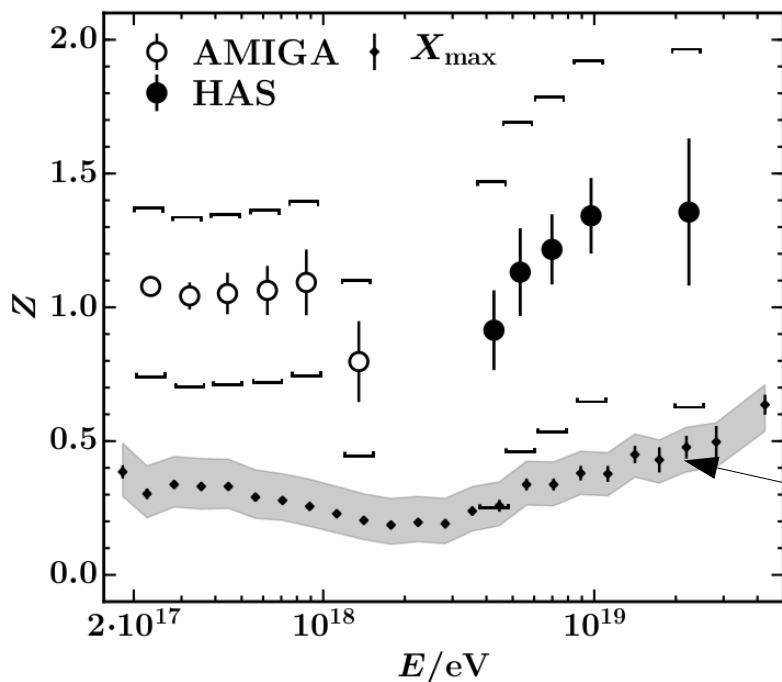
$$Z_{\alpha} = \frac{\langle \ln(\alpha) \rangle - \langle \ln(\alpha) \rangle_p}{\langle \ln(\alpha) \rangle_{Fe} - \langle \ln(\alpha) \rangle_p}$$



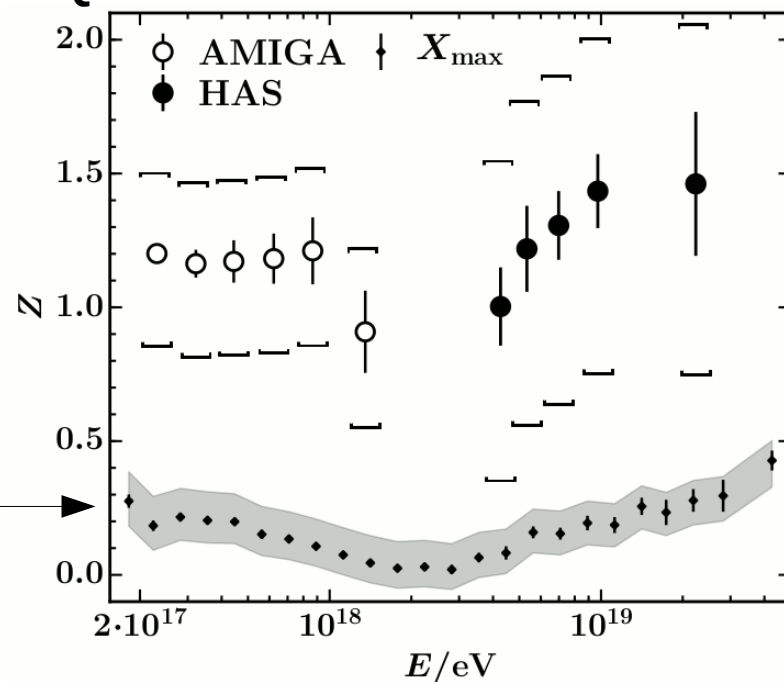
same composition sensitive
observable for

$\left\{ \begin{array}{ll} \text{SD} & \longrightarrow R_{\mu} \\ \text{FD} & \longrightarrow X_{max} \\ \text{UMD} & \longrightarrow \rho_{35} \end{array} \right.$

EPOS

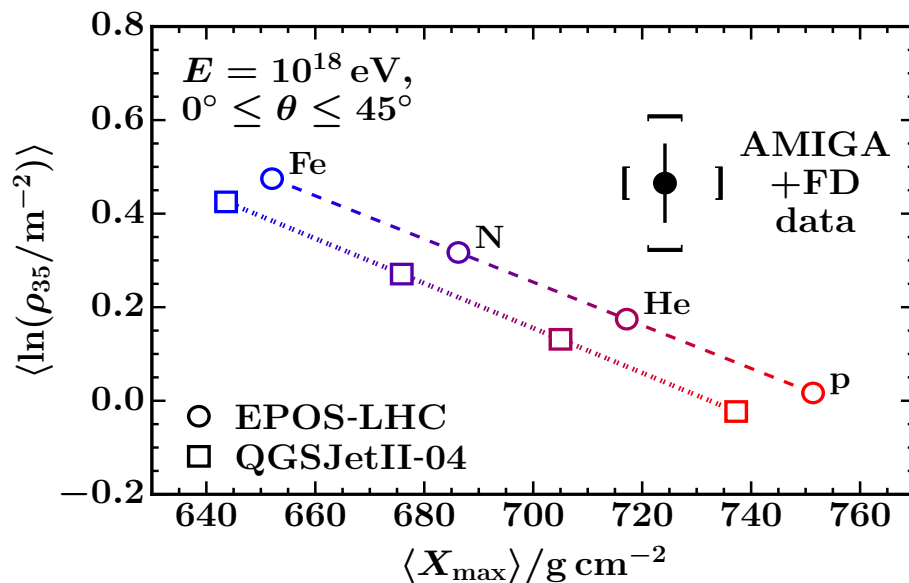
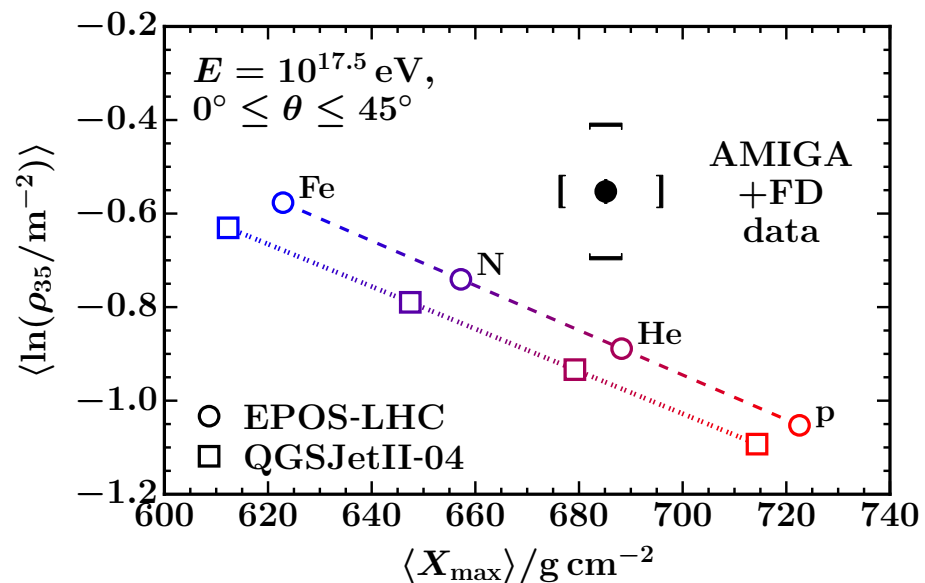


QGSJet



Comparison with other Auger measurements II

Bi-parametric analysis: X_{max}, ρ_{35}



muon deficits in LHC-tuned hadronic models

@ $10^{17.5} \text{ eV}$

EPOS 38%

QGSJet 50%

@ $10^{18.0} \text{ eV}$

EPOS 38%

QGSJet 53%

Final remarks

- ✓ An engineering array for the Underground Muon Detector (UMD) was fully operative at the Pierre Auger Observatory and was used to thoroughly validate the detection system
- ✓ For the production phase several hardware improvements were implemented (see PoS(ICRC2019)202 in the poster session)
- ✓ The first direct observations of a device dedicated exclusively to measuring the muonic component of EAS were presented
- ✓ In the energy range 3×10^{17} eV to 2×10^{18} eV simulations fail to reproduce muon densities even for LHC-tuned hadronic interaction models
- ✓ Compared to data, the combined analysis of X_{max} , ρ_{35} showed a discrepancy ranging from 38% to 53% depending on the model
- ✓ The combined muon analysis at high (SD) and low (UMD) energies match the trend in composition observed with the FD in the whole energy range